Escola de Primavera de Transição e Turbulência
Blumenau 2020

ABCM Associação Brasileira de Engenharia e Ciências Mecânicas

12th Spring School on Transition and Turbulence
September 21th-25th, 2020, Blumenau, SC, Brazil

EPTT2020-0001
ASSESSMENT OF TURBULENT INLET CONDITIONS AND NUMERICAL PARAMETERS ON LES SIMULATIONS OF THE FLOW OVER A SINGLE CYLINDER

Matheus Rover Barbieri
Raissa de Souza Lazzaris
Leonardo Machado da Rosa
Jonathan Utzig
Henry França Meier
Chemical Engineering Department, University of Blumenau
São Paulo St., 3250, I-303 – 89030-000 Blumenau – Santa Catarina – Brazil
matheus_rover@hotmail.com
raissalazzaris.lazzaris@gmail.com
lmrosa@furb.br
jutzig@furb.br
meier@furb.br

Abstract. *The study of flow-induced vibrations has received special attention in the past years, motivated by the occurrence of financial losses and failures in industrial units. Flow structures exert forces over the tubes, whose action is one of the major factors impacting the integrity of equipments. The rise of numerical methodologies enabled the evaluation of such factors in a safer and more economical way. Among the numerical parameters that influence the forces and flow responses in such assessments, the turbulent intensity at the inlet boundary can increase cylinders' oscillation and change velocity profiles and force coefficients. Hence, models able to synthesize the turbulence in numerical simulations are an alternative to represent the flow in a more reliable way. The aim of the present study is to investigate the use of turbulence synthesizer models to approximate from data acquired in an experimental facility, comparing force coefficients and flow features. The results were compared with experimental and literature data. The simulations employing the turbulence synthesizer models presented closer responses regarding the vortex-shedding frequency and the fluctuating lift coefficient. However, the simulation without turbulence synthesizer showed better results for the mean drag coefficient and other flow features, such as the formation length.*

Keywords: *computational fluid dynamics, LES simulation, turbulent inlet conditions, single cylinder.*

1. INTRODUCTION

Flow-induced vibration is a result of the two-way interaction between the fluid forces and the surface reactions of the bluff bodies, existing several situations in which they can happen. The occurrence of such vibrations in industrial equipments is undesirable, once they can compromise the structural integrity of the equipment. Reaching this condition can lead to excessive noise and structural failure, causing financial losses to the industries and eventually harming people and the environment (Blevins, 1990; Bearman, 2011).

The study of the flow over a cylinder is a remarkable case study in the literature (Breuer, 1998; Norberg, 2003, Griffith *et al*., 2011). Flow patterns, force coefficients and frequencies associated to the flow have been widely investigated in the past decades, once they characterize many engineering applications in industries (Goyder, 2002). With the development of numerical methodologies capable of representing physical phenomena, Computational Fluid Dynamics (CFD) became an important technique to study of the flow over cylinders, once it enabled the analysis of flow behavior and force coefficients without conducting physical experiments, as long as the numerical model is validated. The knowledge of the forces acting over cylinders and the flow characteristics are key parameters in the industrial equipments design and enhancement, provided that such information allows for structural design analysis, reducing the occurrence of problems.

In this context, the choice of an appropriate turbulence model, modeling approach and computational domain, such as Unsteady Reynolds-Averaged Navier-Stokes (URANS) and Large Eddy Simulation (LES) models (Moukaled, Mangani and Darwish, 2015) is of great importance, once flow separation and transition to turbulence occur (Silva *et al*., 2017). It has been shown that only models that resolve at least part of the turbulent eddies present good results to the flow over a cylinder (Silva, Utzig and Meier, 2016). Consequently, URANS models are compromised due to the

proximity between the greatest turbulent vortices time scale and the shedding vortex frequency. Based on that, despite its higher computational cost due to the finer mesh required to solve at least the large turbulent eddies, the LES approach is usually applied to resolve the tridimensional turbulent flow over bluff bodies (Lübcke *et al*., 2001; Lam *et al*., 2010; Prsic *et al*., 2014).

Several parameters influence the forces and flow responses. Among them, flow features upstream the cylinder, such as high turbulent intensity at the inlet boundary condition, which can cause a drastic increase in cylinder's oscillation due to the higher energy transferred by the flow, modifying velocity profiles and force statistics (Charreton, *et al*., 2015; de Pedro *et al*., 2016; Palomar and Meskell, 2018). The mean force coefficients and its fluctuations are significantly affected by the free-stream turbulence, increasing for certain turbulent intensities and decreasing for others (King, 1977; Sarpkaya, 1979). Tørum and Anand (1985) found experimentally that drag coefficient values increased for turbulent intensities measured at the pipe location from 3.4% to 5.5% and increased again at an intensity value of 9.5%. Jubran, Hamdan and Bedoor (1993) studied the effects of different turbulent intensities, obtained at the position of the test tube, on the cylinder oscillation and found a higher motion amplitude at the lower turbulent intensity practiced (0.2%). It decreased as the turbulent intensity increased to 2.8% and 3.5% and increased again at higher turbulent intensities (4.2%). Besides, the increase in the turbulent intensity delays the beginning of oscillations in the vortex-shedding excitation region.

An experimental facility is available to the authors of the present work to carry out experimental studies of the flow over cylinders. According to preliminary measurements conducted with Laser Doppler Anemometry (LDA) technique, a turbulent intensity of 10.1% at the channel inlet was found, which is high compared to the values in the order of 1% considered in most of the studies in the literature (Tørum and Anand, 1985; Lam *et al*., 2004; Kumar, *et al*., 2009; Lam *et al*., 2010). Although this high turbulent intensity has not affected flow patterns and frequencies associated to the flow, previous studies conducted by the research group showed discrepancies mainly in the numerical calculations of force coefficients and velocity profiles (Silva *et al*., 2017; Barbieri, *et al*., 2019).

Accordingly, the turbulence condition at the inlet can be represented in numerical simulations by models capable of synthesizing it. Therefore, the present study aims to investigate the effects of using turbulence synthesizer models as boundary condition at the domain inlet. The Random Flow Generator model and the Vortex Method model were compared to a standard simulation with a constant velocity field normal to the boundary. The turbulence synthesizer models parameters were set similarly to the experimental data acquired in the experimental facility, in order to validate the numerical models. Furthermore, force coefficients, flow characteristics, velocity profiles and frequencies associated to the flow were used for evaluating the performance of the LES approach.

2. MATHEMATICAL MODELS AND METHODOLOGY

According to previous studies conducted by the research group, the flow in the experimental facility presents a high turbulent intensity at the channel inlet (Silva *et al*., 2018). This condition leads to challenges on the velocity profiles validation downstream the cylinder, as well as the force coefficients and flow features. Hence, numerical studies employing turbulence synthesizer methods at the inlet boundary condition were conducted, considering the confined flow in a channel over a cylinder of a diameter D = 1 cm. The channel domain in the simulations has the inlet boundary condition set at 15 cm upstream the cylinder (15D) and the outlet boundary condition 30 cm downstream the cylinder (30D). The width of the channel has 8 cm (8D) and the height of the channel in the computational domain is 5.25D, half of the height of the experimental channel, where a symmetry boundary condition was adopted at the top wall as a geometric simplification, as shown in Figure 1. This simplification allows for computational and time resources savings and provides results close to the full domain simulation (Silva *et al*., 2017).

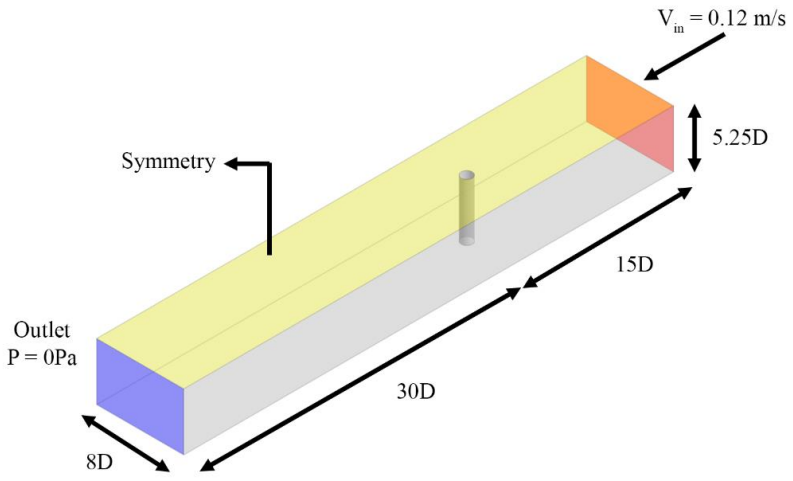

Figure 1. Geometric characteristics and boundary conditions.

At the inlet boundary condition, a fixed velocity V_{in} = 0.12 m/s was specified resulting in a Reynolds number calculated to the cylinder diameter $\mathrm{Re}_D = V_{\mathrm{in}} D/\nu = 1200$, where ν is the kinematic viscosity of the fluid. The outlet boundary condition was set as static pressure P = 0 Pa. All the remaining boundaries were set as walls with no-slip condition.

The finite volume method implemented in the commercial code ANSYS Fluent 19.0 with the physical properties of liquid water (ρ = 998.2 kg/m³; ν = 1×10^{-5} m²/s) was used to solve the filtered three-dimensional incompressible Navier-Stokes equations for a Newtonian fluid, represented in Eq. (1) and Eq. (2):

$$\frac{\partial \bar{u}_i}{\partial x_i} = 0, \tag{1}$$

$$\frac{\partial \bar{u}_i}{\partial t} + \frac{\partial \bar{u}_i \bar{u}_j}{\partial x_j} = \frac{\partial}{\partial x_j}\left[\nu\left(\frac{\partial \bar{u}_i}{\partial x_j} + \frac{\partial \bar{u}_j}{\partial x_i}\right)\right] - \frac{1}{\rho}\frac{\partial \bar{P}}{\partial x_i} - \frac{\partial \tau_{ij}}{\partial x_j}, \tag{2}$$

where $\bar{u}_i$ are the filtered velocity components, x_i are the cartesian coordinates, ρ is the density of the fluid and $\bar{P}$ is the filtered pressure. The subgrid-scale Reynolds Stress tensor τ_{ij} includes the effects of small scales in the flow, and it was modeled with the Dynamic LES turbulent approach (Germano, *et al*., 1991) for all cases.

Hexahedral grids were generated with 192 cells along with the cylinder perimeter. The node closest to the cylinder and channel walls is located at 0.03 mm, which provided y^+ values smaller than 1. The maximum cell size is 1.25 mm within 3 cm from the cylinder, expanding up to 2.50 mm at the inlet and outlet faces. The mesh size was 2,337,523 nodes. The pressure-velocity coupling was solved with SIMPLEC method, with the bounded central differencing momentum discretization and second order implicit transient formulation. The time step was fixed in 1×10^{-4} s, ensuring a Courant number inferior to 1. Averages were acquired for at least 8 s after the flow stabilization, taking about 3 weeks for the Case 1, simulated in 12 parallel processes using AMD Opteron Processor 6366 HE processors at 1,8 GHz.

The simulations followed the base configuration defined in Case 1. From this setup, simulations parameters such as turbulent inlet conditions and numerical parameters were varied. The following simulation configurations were set up:

- **Case 1**: This case employs a Large Eddy Simulation with the Dynamic Smagorinsky-Lilly Model, in which the Smagorinsky model constant (C_s) varies in time and space, removing the need for the user to specify the model constant. The procedure relies on the application of a second filter (test filter) of width $\hat{\Delta}$ to the motion equations, which is twice the grid filter width Δ. At the test filtered field level, the subgrid-scale stress tensor can be expressed according to Eq. (3):

$$T_{ij} = \widehat{\rho u_i u_j} - \left(\widehat{\rho u_i}\widehat{\rho u_j}/\hat{\bar{\rho}}\right). \tag{3}$$

Assuming scale similarity, both T_{ij} and τ_{ij} are modeled in the same way with the Smagorinsky-Lilly model, as presented in Eq. (4) and Eq. (5):

$$\tau_{ij} = -2C\bar{\rho}\Delta^2\left|\tilde{S}\right|\left(\tilde{S}_{ij} - \frac{1}{3}\tilde{S}_{kk}\delta_{ij}\right), \tag{4}$$

$$T_{ij} = -2C\hat{\bar{\rho}}\hat{\Delta}^2\left|\hat{\tilde{S}}\right|\left(\hat{\tilde{S}}_{ij} - \frac{1}{3}\hat{\tilde{S}}_{kk}\delta_{ij}\right). \tag{5}$$

The C coefficient is assumed to be the same in Eq. (4) and Eq. (5), which is related to $C = C_s^2$. The grid filtered and the test-filtered subgrid-scales are related by the Germano identity given by Eq. (6):

$$\mathcal{L}_{ij} = T_{ij} - \widehat{\tau_{ij}} = \widehat{\bar{\rho}\tilde{u}_i\tilde{u}_j} - \frac{1}{\hat{\bar{\rho}}}\left(\widehat{\bar{\rho}\tilde{u}_i}\widehat{\bar{\rho}\tilde{u}_j}\right), \tag{6}$$

where $\mathcal{L}_{ij}$ is obtained from the resolved large eddy field. The expression to solve for C can be obtained from substituting the grid-filter Smagorinsky-Lilly model and Eq. (5) into Eq. (6), with the contraction obtained from the least square analysis of Lilly (1992), resulting in Eq. (7):

$$C = \frac{\left(\mathcal{L}_{ij} - \mathcal{L}_{kk}\delta_{ij}/3\right)}{M_{ij}M_{ij}}, \tag{7}$$

with

$$M_{ij} = -2\left(\hat{\Delta}^2\hat{\rho}\left|\hat{\tilde{S}}\right|\hat{\tilde{S}}_{ij} - \Delta^2\bar{\rho}|\tilde{S}|\tilde{S}_{ij}\right). \tag{8}$$

The inlet boundary condition consists in a constant velocity, normal to the boundary. The simulations were conducted without under-relaxation factor and with convergence criteria of 1×10^{-5} for all variables. Based on this simulation setup, turbulent inlet conditions were evaluated.

- **Case 2**: The Random Flow Generator (RFG) model from Smirnov *et al*. (2001) was studied for the geometry and operating conditions of the experimental facility. The inlet boundary condition was configured with turbulent imitating perturbations given by the RFG. In this method, fluctuating velocity components are computed by synthesizing a divergence-free velocity-vector field from the summation of Fourier harmonics. A turbulent intensity of 10.1% and a turbulence length scale of 5.02 mm were set, both estimated based on experimental measurements obtained with Laser Doppler Anemometry (LDA) technique in the experimental facility. Further configurations were kept the same as the Case 1.

- **Case 3**: The inlet boundary condition was configured with a velocity fluctuation algorithm given by the Vortex Method in this case. This time-dependent inlet condition consists in a random two-dimensional vortex method, in which a perturbation is added on a specified mean velocity profile through a fluctuating vorticity field. It is based on the Lagrangian form of the two-dimensional vorticity evolution equation and the Biot-Savart law. A particle or a "vortex-point" is convected randomly and carry information about the vorticity field. The circulation Γ_i and an assumed spatial distribution η represent the amount of vorticity carried by a given particle i, based on a number of vortex points N and the area A of the inlet section (Mathey *et al*., 2006), according to Eq. (9) and Eq. (10):

$$\Gamma_i(x,y) = 4\sqrt{\frac{\pi A k(x,y)}{3N[2\,ln(3) - 3ln\,(2)]}}, \tag{9}$$

$$\eta(x_i) = \frac{1}{2\pi\sigma^2}\left(2e^{-|x|^2/2\sigma^2} - 1\right)2e^{-|x|^2/2\sigma^2}, \tag{10}$$

where k is the turbulent kinetic energy. The parameter σ provides control over the size of a vortex particle. The resulting discretization of the velocity field is given by Eq. (11):

$$u_i(x_i) = \frac{1}{2\pi}\sum_{i=1}^{N}\Gamma_i\frac{[(x_i - x_i)\times z_i]\left(1 - e^{|x_i - x_i'|^2/2\sigma^2}\right)}{\left|x_i - x_i'\right|^2}, \tag{11}$$

where x_i is the unit vector in the streamwise direction. σ is calculated according to a known profile of mean turbulent kinetic energy and mean dissipation rate at the inlet as stated in Eq. (12):

$$\sigma = \frac{k^{3/2}}{2\varepsilon}. \tag{12}$$

The sign of each vortex circulation is changed randomly each characteristic time scale, which consists in the time necessary for a two-dimensional vortex convected by the bulk velocity in the boundary normal direction to travel along n times its mean characteristic two-dimensional size. The vortex method considers only velocity fluctuations in the plane normal to the streamwise direction. If the mean streamwise velocity U is considered a passive scalar, the fluctuation u' resulting from the transport of U by the planar fluctuating velocity field v' is modeled by Eq. (13) (Mathey *et al*., 2003):

$$u' = -\bar{v}' \cdot g_i, \tag{13}$$

where g_i is the unit vector aligned with the mean velocity gradient $\overrightarrow{\nabla U}$. A random perturbation is considered if the mean velocity gradient is equal to zero.

For the present work, a number or vortex points N equal to 200, a turbulent intensity of 10.1% and a turbulent length scale of 5.02 mm were set. Further configurations were the same as the Case 1.

3. RESULTS AND DISCUSSION

Table 1 show the main flow features and force coefficients responses for each case. The data line named Experiments comprises flow features (L_f/D and St) obtained by previous works conducted by the research group at LFC/LVV at FURB (Silva *et al*., 2018), while the force coefficients ($\bar{C}_D$ and C_L') are results from other authors. In comparison with the experimental data, the Case 1 showed a good agreement of the formation length (L_f/D), which consists in the distance between a point in the center of the cylinder (radius equal to zero) and the minimum velocity point in the streamwise direction. However, there was an overprediction on the mean velocity profile in the streamwise direction (U/V_{in}) in the vortex street region, as well as the crosswise velocity fluctuation (w'/V_{in}), as observed in Figure 2 and Figure 3, respectively. Nonetheless, vortex formation and detachment dynamic are well presented, according to the agreement of the Strouhal number ($St = fD/V_{in}$, where f is the vortex shedding frequency) within the range $0.20 < St < 0.23$ (Blevins, 1990).

Although the numerical studies of Franke and Frank (2002), Prsic *et al.* (2014) and the simulations from the this work fit in the subcritical Reynolds regime, which ranges from $200 < Re < 100000$ (Sumer and Fredsøe, 1997), slight discrepancies were observed for the force coefficients and flow characteristics. In general, the present results showed higher values for the mean drag coefficient, formation length and Strouhal number, while the fluctuating component of the lift coefficient was smaller compared to the LES simulation of Prsic *et al.* (2014).

Table 1. Force coefficients and flow features for the different cases

Case	$\bar{C}_D$	C_L'	L_f/D	St
Experiments	0.98±0.05[1]	0.083[2]	1,85[3]	0.200[3]
LES Franke e Frank (2002)	0.978	-	1.64	0.209
LES Prsic *et al*. (2014)	1.078	0.195	1.27	0.215
Case 1 (base)	1.157	0.058	1.86	0,230
Case 2 (Vortex Method)	1.171	0.088	1.68	0.225
Case 3 (RFG)	1.161	0.084	1.74	0.220

[1] Breuer (1998); [2] Correlation from Norberg (2003); [3] Silva *et al*. (2018).

The results showed small variations for the majority of the global parameters for Case 1 and Case 3, but an increase was observed for Case 3 regarding the fluctuation of the streamwise velocity u', which is the component in the same direction of the drag force, as can be seen in Figure 2. The results in Table 1 also show minor influence of the model over the vortex detachment dynamic, indicated by the similar Strouhal numbers. The influence of this model is stronger in the streamwise velocity and, therefore, in the fluctuation of the drag force, approximating the u' profile to the experimental results obtained with LDA in the recirculation region ($0 < x/D < 1.85$). The Case 3 also promoted a smoothing of the U/V_{in} profile, but with a bigger minimum velocity compared to those without the RFG model or in the experimental profile, as can be seen in Figure 2. Although some flow characteristics observed for Case 3 are closer to the experimental results, mainly regarding velocity profiles, the computational cost is twice bigger than Case 1.

Similar results regarding the force coefficients and flow parameters were obtained between employing the RFG and the Vortex Method models. Regarding the mean velocity profiles and their fluctuations, Case 2 was able to accurately predict their behavior, except for the mean velocity in the streamwise direction (U/V_{in}), evidenced by a shorter recirculation length (L_f/D), a more pronounced minimum velocity, as well the overprediction of the mean velocity profile in the vortex street, according to Figure 2. Both the simulations Case 2 and Case 3, due to the turbulence synthetization at the domain inlet, presented a remarkably higher computational cost compared with the Case 1, needing twice the time of Case 1 with the same computational cores.

Figure 3 shows the mean and fluctuation components of the crosswise velocity for the different cases. Close to the cylinder, in a distance up to 4D downstream to it, the effect of the lift force acting over the tube is more pronounced,

representing the formation and detachment of vortices. As long as these fluid structures flow downstream, they lose vorticity and the mean crosswise velocity tends to zero at high distances from the cylinder. Regarding the fluctuation of the crosswise velocity in Figure 3 (right), there are small discrepancies between the simulations and the experimental data up to the formation length and at high distances from the cylinder. However, Case 1 and Case 3 presented overprediction of the crosswise velocity maximum fluctuation.

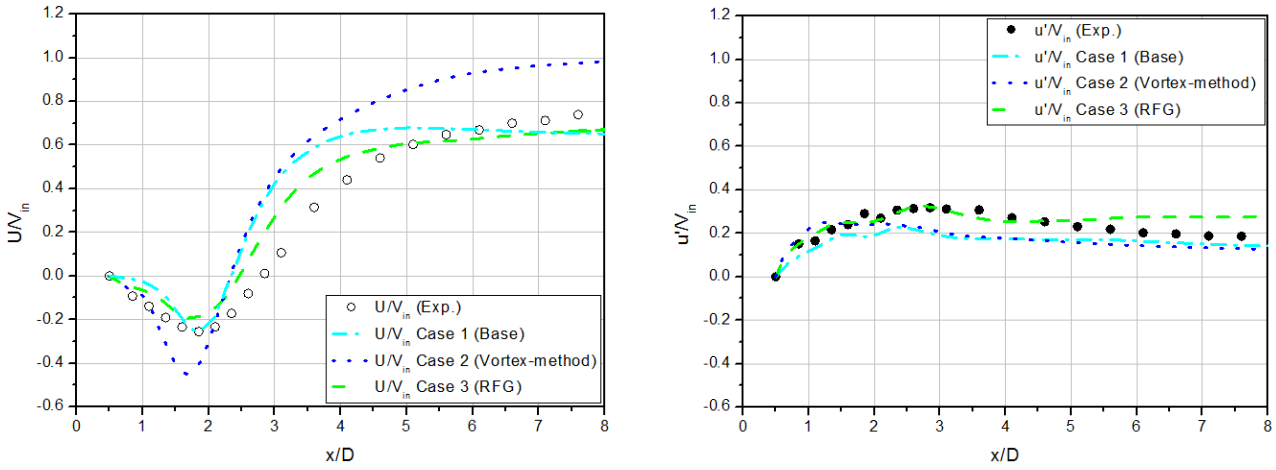

Figure 2. (Left) Mean velocity and (right) mean velocity fluctuation of the streamwise velocity in the flow direction. Experimental data from Silva *et al*. (2018).

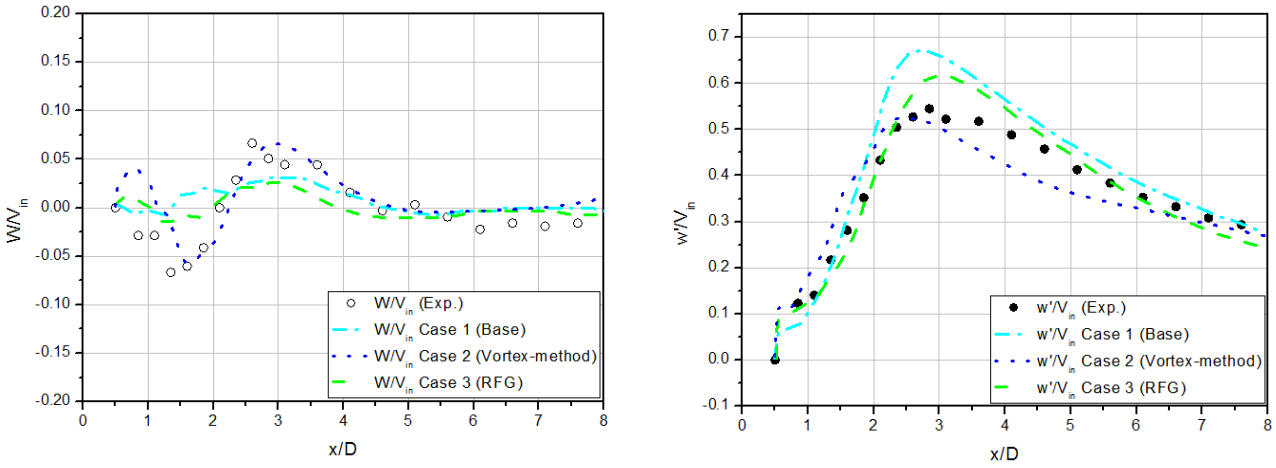

Figure 3. (Left) Mean velocity and (right) mean velocity fluctuation of the crosswise velocity in the flow direction. Experimental data from Silva *et al*. (2018).

4. CONCLUSION

The CFD technique allowed for the evaluation of flow phenomena, seeking to represent the physics of the problem in a reliable way. The present work studied different turbulence synthesizer methods at the inlet boundary condition, aiming to obtain data regarding flow features, force coefficients and frequencies associated to the flow. These data were compared with other numerical studies in the literature, as well as experimental data. The turbulence synthesizer methods showed some responses closer to experimental data and results found in the literature, such as better agreement in the fluctuating lift coefficient and the Strouhal number in comparison with the simulation without turbulence synthesizer method. However, they presented a worse performance on representing the mean drag coefficient and the formation length. Despite their better representation of some responses, the higher computational cost required to conduct such simulations with turbulence synthesizer methods justify their use only if computational resources allow for it.

5. ACKNOWLEDGEMENTS

This study was financed by CAPES – Financial code 001. The authors would like to acknowledge the financial support from Petróleo Brasileiro S.A. (PETROBRAS) through the cooperation agreement 5850.0103010.16.9 and CNPq (Process 308714/2016-4).

6. REFERENCES

Barbieri, M. R.; Silva, B. L.; Catapan, J.; Lazzaris, R. S.; Utzig, J.; Meier, H. F., 2019. "Numerical study of the crossflow over different body geometries". *Presented at the IV Simpósio Paranaense de Modelage, Simulação e Controle de Processos – SIMPROC*, Curitiba, Brazil.

Bearman, P. W., 2011. "Circular cylinder wakes and vortex-induced vibrations". *Journal of Fluids and Structures*, Vol. 27, pp. 648-658.

Blevins, R. D.,1990. *Flow-induced vibration*. Van Nostrand Reinhold, New York, 2nd edition.

Breuer, M., 1998. "Numerical and modeling influences on large eddy simulation for the flow past a circular cylinder". *International Journal of Heat and Fluid Flow*, Vol. 19, pp. 512-521.

Charreton, C.; Béguin, C.; Yu, K. R.; Étienne, S., 2015. "Effect of Reynolds number on the stability of a single flexible tube predicted by the quasi-steady model in tube bundles". *Journal of Fluids and Structures*, Vol. 56, pp. 107-123.

De Pedro, B.; Parrondo, J.; Meskell, C.; Oro, J. F., 2016. "CFD modelling of the cross-flow through normal triangular tube arrays with one tube undergoing forced vibrations or fluidelastic instability". *Journal of Fluids and Structures*, Vol. 64, pp. 67-86.

Franke, J. and Frank, W., 2002. "Large eddy simulation of the flow past a circular cylinder at $Re_D = 3900$". *Journal of Wind Engineering and Industrial Aerodynamics*, Vol. 90, pp. 1191-1206.

Germano, M.; Piomelli, U.; Moin, P.; Cabot, W. H., 1991. "A dynamic subgrid-scale eddy viscosity model". *Physics of Fluids A*, Vol. 3, pp. 1760-1765.

Goyder, H. G. D., 2002. "Flow-induced-vibration in heat exchangers". *Chemical Engineering Research and Design*, Vol. 80, pp. 226-232.

Griffith, M. D.; Leontini, J.; Thompson, M. C.; Hourigan, K., 2011. "Vortex shedding and three-dimensional behavior of flow past a cylinder confined in a channel". *Journal of Fluids and Structures*, Vol. 27, pp. 855-860.

Jubran, B. A.; Hamdan, M. N.; Bedoor, B. A., 1993. "Interference and turbulence intensity effect on the flow-induced vibration of smooth and rough cylinders". *Journal of Fluids and Structures*, Vol. 7, pp. 457-470.

King, R., 1977. "A review of vortex-shedding research and application". *Ocean Engineering*, Vol. 4, pp. 141-171.

Kumar, R. A.; Sohn, C. H.; Gowda, B. H. L., 2009. "Influence of corner radius on the near wake structure of a transversely oscillating square cylinder". *Journal of Mechanical Science and Technology*, Vol. 23, pp. 2390-2416.

Lam, K.; Wang, F. H.; Li, J. Y.; So, R. M. C., 2004. "Experimental investigation of the mean and fluctuating forces of wavy (varicose) cylinders in a cross-flow". *Journal of Fluids and Structures*, Vol. 19, pp. 321-334.

Lam, K.; Lin, Y. F.; Zou, L.; Liu, Y., 2010. "Experimental study and large eddy simulation of turbulent flow around tube bundles composed of wavy and circular cylinder". *International Journal of Heat and Fluid Flow*, Vol. 31, pp. 32-44.

Lilly, D. K., 1992. "A proposed modification of the Germano subgrid-scale closure method". *Physics of Fluids A*, Vol. 4, pp. 633-635.

Lübcke, H.; Schmidt, St.; Rung, T.; Thiele, F., 2001. "Comparison of LES and RANS in bluff-body flows". *Journal of Wind Engineering and Industrial Aerodynamics*, Vol. 89, pp. 1471-1485.

Mathey, F.; Cokljat, D.; Bertoglio, J.P.; Sergent, E., 2003. "Specification of LES Inlet Boundary Condition using Vortex Method". In4 *4th International Symposium on Turbulence, Heat and Mass Transfer*. Antalaya, Turkey. Begell House, Inc.

Mathey, F.; Cokljat, D.; Bertoglio, J.P.; Sergent, E., 2006. "Assessment of the vortex method for Large Eddy Simulation inlet conditions". *Progress in Computational Fluid Dynamics*, Vol. 6, pp. 58-67.

Moukaled, F.; Mangani, L.; Darwish, M., 2015. *The Finite Volume Method in Computational Fluid Dynamics: An advanced introduction with OpenFOAM® and Matlab (Fluid Mechanics and its applications).* Springer – Verlag, Switzerland, 1st edition, v. 113 of Fluid Mechanics and its Applications.

Norberg, C., 2003. "Fluctuating lift on a circular cylinder: review and new measurements". *Journal of Fluids and Structures*, Vol. 19, pp. 57-96.

Sarpkaya, T., 1979. "Vortex-induced oscillations: A selective review". *Journal of Applied Mechanics*, Vol. 46, pp. 241-258.

Palomar, B. P. and Meskell, C., 2018. "Sensitivity of the damping controlled fluidelastic instability threshold to mass ratio, pitch ratio and Reynolds number in normal triangular arrays". *Nuclear Engineering and Design*, Vol. 331, pp. 32-40.

Prsic, M. A.; Ong, M. C.; Pettersen, B.; Myrhaug, D., 2014. "Large Eddy Simulation of flow around a smooth circular cylinder in a uniform current in the subcritical flow regime". *Ocean Engineering*, Vol. 77, pp. 61-73.

Silva, B. L.; Barbieri, M. R.; Utzig, J.; Martignoni, W. P.; Meier, H. F., 2017. "On the influence of spanwise boundary conditions on the Large Eddy Simulation of the flow past a single cylinder". *Presented at the 2017 AIChE Annual Meeting*. Minneapolis, USA.

Silva, B. L.; Luciano, R. D.; Utzig, J.; Meier, H. F., 2018. "Flow patterns and turbulence effects in large cylinder arrays". *International Journal of Heat and Fluid Flow*, Vol. 69, pp. 136-149.

Silva, B. L.; Utzig, J.; Meier, H., 2016. "CFD-based design of experiments for the study of flow-induced vibrations in a tube bundle". In *Proceedings of the 10th ABCM Spring School on Transition and Turbulence – EPTT2016*. São José dos Campos, Brazil.

Smirnov, R.; Shi, S.; Celik, I., 2001. "Random Flow Generator for Large Eddy Simulation and Particle-Dynamics Modeling". *Journal of Fluid Engineering*, Vol. 123, pp. 359-371.

Sumer, B.M. and Fredsøe, J., 1997. "Hydrodynamics around cylindrical structures". *Advanced Series on Ocean Engineering*, Vol. 12. World Scientific.

Tørum, A. and Anand, N. M., 1985. "Free span vibration of submarine pipelines in steady flows – effect of free-stream turbulence on mean drag coefficients". *Journal of Energy Resources Technology*, Vol. 107, pp. 415-420.

7. RESPONSIBILITY NOTICE

The authors are the only responsible for the printed material included in this paper.